Materials Chemistry and Physics 245 (2020) 122762

Contents lists available at ScienceDirect

Materials Chemistry and Physics

journal homepage: www.elsevier.com/locate/matchemphys

PMAO-assisted thermal decomposition synthesis of high-stability ferrofluid based on magnetite nanoparticles for hyperthermia and MRI applications

Thi Kim Oanh Vuong [a,f,*], The Tam Le [b], Hai Doan Do [a], Xuan Truong Nguyen [a], Xuan Ca Nguyen [c], Thi Thu Vu [d], Trong Lu Le [e], Dai Lam Tran [e,f]

[a] Institute of Materials Science, Vietnam Academy of Science and Technology, 18 Hoang Quoc Viet Road, Hanoi, Viet Nam
[b] Vinh University, 182 Le Duan, Vinh, Viet Nam
[c] Department of Physics and Technology, TNU - University of Sciences, Viet Nam
[d] University of Science and Technology of Hanoi, Vietnam Academy of Science and Technology, 18 Hoang Quoc Viet Road, Hanoi, Viet Nam
[e] Institute for Tropical Technology, Vietnam Academy of Science and Technology, 18 Hoang Quoc Viet Road, Hanoi, Viet Nam
[f] Graduate University of Science and Technology, Vietnam Academy of Science and Technology, 18 Hoang Quoc Viet Road, Hanoi, Viet Nam

HIGHLIGHTS

- Fe3O4 magnetic nanoparticles were synthesized by thermal decomposition method.
- Fe3O4@PMAO ferrofluids revealed excellent colloidal stability over 6 storage months.
- The SAR of 66.04 W.g-1 was obtained at ferrofluid concentration of only 5 mg.mL-1.
- T2-weighted intensity in ferrofluid-injected tissues was increased by 5.85 times.

GRAPHICAL ABSTRACT

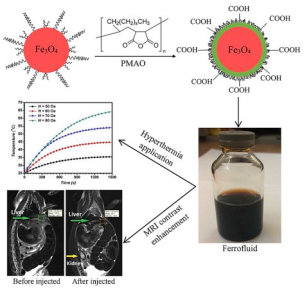

ARTICLE INFO

Keywords:
Ferrofluid
Thermal decomposition
MRI
Hyperthermia
Non-invasive cancer treatment

ABSTRACT

The combination of magnetic fluid hyperthermia and magnetic resonance imaging is recently considered to be one of the most promising non-invasive cancer treatment. In this work, a highly stable ferrofluid based on magnetite nanoparticles with high magnetization and high specific absorption rate will be developed. The ferrofluid was synthesized by thermal decomposition using poly (maleic anhydride-alt-1-octadecene, noted as PMAO) as a phase transferring ligand. The results have demonstrated that the magnetic particles were fully covered at high coverage by long non-magnetic polymeric chains. The particle size was increased by 25–30% while the saturation magnetization was decreased approximately 7–9% after phase transfer process. Remarkably, the prepared ferrofluid revealed excellent colloidal stability over six months of storage with zeta potentials less than −40 mV. As consequently, a relatively high specific absorption rate of 66 W.g-1 was obtained at ferrofluid concentration of only 5 mg.mL-1. Additionally, high-resolution magnetic resonance images with improved transverse relaxation T2 were observed when using magnetite-based ferrofluid for both *in-vitro* and *in-vivo* tests. This study demonstrates a novel approach for tailoring magnetic nanoparticles applicable in magnetic fluid hyperthermia and imaging of tumor cells.

* Corresponding author. Institute of Materials Science, Vietnam Academy of Science and Technology, 18 Hoang Quoc Viet Road, Hanoi, Viet Nam.
E-mail address: oanhvtk@ims.vast.ac.vn (T.K. Oanh Vuong).

https://doi.org/10.1016/j.matchemphys.2020.122762
Received 22 July 2019; Received in revised form 16 December 2019; Accepted 3 February 2020
Available online 5 February 2020

1. Introduction

Magnetic fluid hyperthermia has been gaining many attentions in cancer therapy over last few decades. In this method, the magnetic suspensions can be delivered to targeting organs, and then generate a local heat (around 41–46 °C) [1] to cause some negative effects or even kill cancer cells. For this, superparamagnetic ferrofluids are extensively studied as potential candidates [2–5] due to their high saturation magnetization and good biocompatibility [6,7]. To better evaluate the hyperthermic ability of a magnetic fluid, specific absorption rate (SAR) [8] which is defined as the rate at which energy is absorbed by the subject exposed to an electromagnetic field can be used. The higher SAR values, the better hyperthermia yield is obtained. It is worthy to notice that there is a limit of the strength as well as frequency of alternating magnetic field in biomedical applications [9]. Therefore, several other factors should be considered to optimize hyperthermia process, such as homogeneity and colloidal stability of the used ferrofluids [10].

Another important application of magnetic nanoparticles (MNP_s) must be taken into account is their use as contrast agents in magnetic resonance imaging (MRI) [11,12]. It is obvious that the combination of hyperthermia (a non-invassive cancer treatment) with MRI (a non-invassive cancer diagnosis) could provide us a novel approach to deal with these deadly diseases at very early stages [13]. Some studies have found that the MNP_s are able to shorten the transverse relaxation time (T_2) of water protons, then enhance T_2-weighted contrast degree, thus improve the quality of MRI images [14]. It was also reported that the monodispersed magnetic particles exhibited higher T_2 relaxation time and lower relaxation rate [14]. Clearly, the MNP_s with good colloidable stability are highly desired to provide magnetite-based contrast agents with high quality.

To improve the colloidal stability of magnetic particles, some agents (i.e, silica, dextran, chitosan, liposomes) [15–17] or some ligands (i.e, folic acid) [18] might be used to hydrophilize their surfaces. Recently, the amphiphilic polymers with a hydrophilic head and a hydrophobic tail have been more preferable for surface modification of magnetic nanoparticles [19,20]. The advantages of using these amphiphilic polymers as phase transferring ligands include possibility to cover almost nanoparticles synthesized in organic solvents and ability to provide extremely high stability. For now, the two most common amphiphilic polymers are 1,2-distearoyl-sn-glycero-3-phosphoethanolamine-N-[amino (polyethylene glycol)-2000] (DSPE - PEG) and poly (maleic anhydride-alt-1-octadecene) (PMAO) [21,22].

In our research group, several ferrofluids based on magnetite nanoparticles have been synthesized by thermal decomposition method using various phase transferring ligands such as sodium dodecyl sulfate (SDS) and poly acrylic acid (PAA) [23,24]. According to our magnetic heating studies, those ferrofluids are applicable for hyperthermia with relatively high SAR values but they seem to be not very stable over time. The best colloidal stability obtained when coating magnetite particles with PAA polymer was still restricted in less than one month. Such short-term stability of ferrofluids remains hindering problem which need to be addressed.

The aim of this work is to develop a highly stable ferrofluid by totally encapsulating magnetite particles with PMAO brushes. The high coverage of such long amphiphilic polymer chains on the surface of nanoparticles might provide stronger steric and electrostatic repulsion that will limit the agglomeration of particles. The structural and magnetic of the as-prepared ferrofluid were studied in details. More importantly, its stability over time was thoroughly monitored by measuring zeta potential. Its ability to be applied in magnetic hyperthermia and MRI contrast enhancement was also examined and discussed.

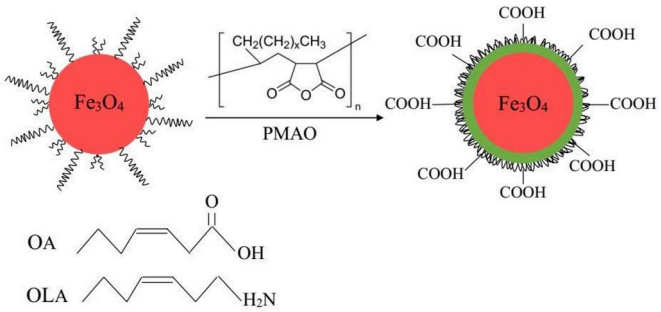

Fig. 1. Transferring mechanism of PMAO@Fe_3O_4 ferrofluids.

2. Methodology

2.1. Chemicals

All reagents used were analytical grade without further purification. Iron (III) acetylacetonate (Fe(acac)3), oleylamine (OLA), oleic acid (OA), and poly (maleic anhydride-alt-1-octadecene) (PMAO) were purchased from Sigma-Aldrich. The Sarcoma. 180 cells for cytotoxicity tests were obtained from American Type Culture Collection (ATCC, USA). The CellTiter kit in MTT assay was purchased from Promega, USA.

2.2. Synthesis of Fe_3O_4 nanoparticles

The protocol for the synthesis of magnetic nanoparticles was described in our previous work [24]. Briefly, a mixture of $Fe(acac)_3$ (0.01 M), oleic acid (0.5 M), and oleylamine (0.5 M) was prepared in dibenzyl ether. The reaction was preceded for 2 h at desired temperatures (265 °C, 285 °C, 298 °C). The obtained precipitates were then washed thoroughly with ethanol, and finally dried at 70 °C. The final products prepared at 265, 285 and 298 °C were denoted as M1, M2, and M3, respectively.

2.3. Preparation of Fe_3O_4 magnetic fluids

The ferrofluid was prepared from as-synthesized magnetic nanoparticles using PMAO as transfer ligand. Fe_3O_4 nanoparticles (200 mg mL^{-1}) were sonicated in n-hexane for 5 min to make sure that the particles were well dispersed. Meanwhile, PMAO (50 mg mL^{-1}) was dissolved in chloroform. The phase transferring process was conducted by dropwising 10 ml of dispersed magnetic nanoparticles into 10 ml PMAO solution at speed of 10 ml min^{-1}. Once the phase transfer is finished, the reaction mixture was let to dry at room temperature until no more organic solvents are found. Finally, 10 ml of 0.05 M sodium hydroxide solution was added to the residue to obtain the aqueous ferrofluid. The post-phase transferred samples were labeled as L1@PMAO, L2@PMAO and L3@PMAO corresponding to the initial dried samples of M1, M2 and M3. The transferring process is illustrated in Fig. 1.

2.4. Morphology and magnetic behaviors of magnetic ferrofluids

The morphology of the samples was examined using transmission electron microscopy (TEM; JEOL JEM-1010) operating at 50 kV. The particle size distribution and polydispersity index (PDI) of the magnetic fluids were determined by the dynamic light scattering (DLS) technique whereas their surface charges in water were measured by zeta potential measurements using Zetasizer (Nano ZS, Malvern, UK). The saturation magnetization of the samples at room temperature was measured under the highest magnetic field of 10 kOe using a home-made vibrating sample magnetometer (VSM).

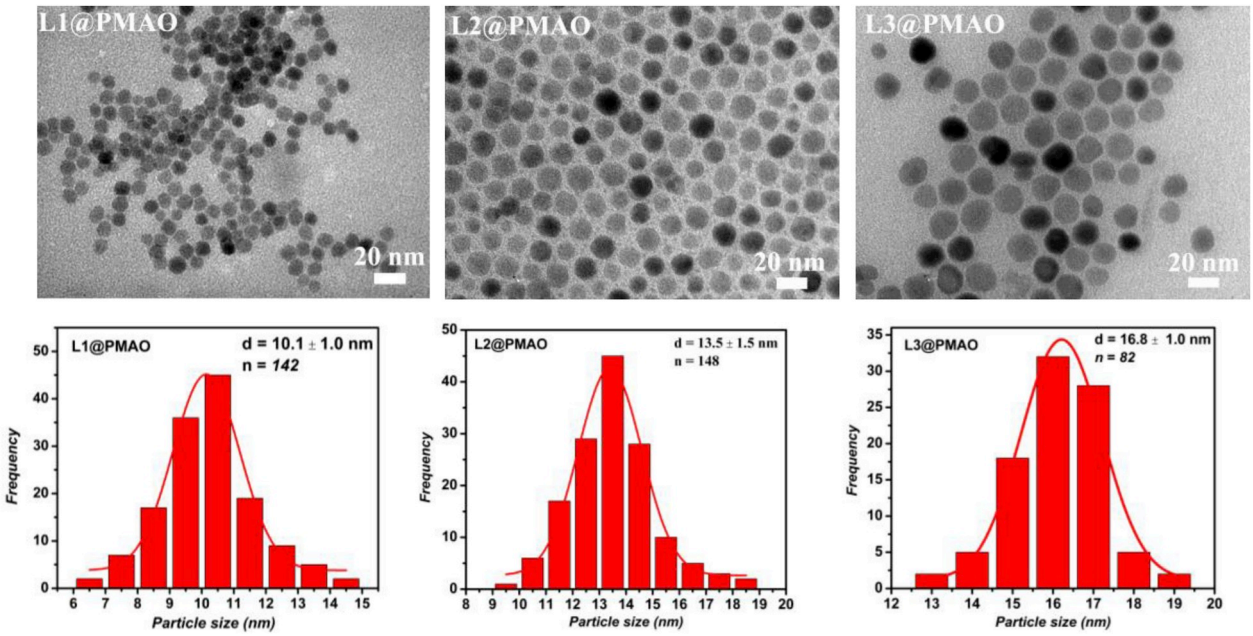

Fig. 2. TEM images and size distribution diagrams of three post-phase transfer samples: L1@PMAO, L2@PMAO and L3@PMAO.

2.5. In vitro cytotoxicity test by MTT assay method

The cytotoxic effect of L3@PMAO on Sarcoma. 180 cells (cancer cells) was tested by MTT [(3-(4,5-dimethylthiazol-2-yl)-2,5-diphenyl tetrazolium bromide] assay using CellTiter kit. The MTT assay provides fast and convenient assay with great sensitivity applicable for drug screening at massive scale [25,26]. The detailed toxicity study was done at Nano-Biotechnology and Application Unit, Vietnam National University, Hanoi, Vietnam.

2.6. Magnetic induction heating

The effects of magnetic induction heating on the optimized magnetite ferrofluid sample (L3@PMAO) were investigated under an alternating magnetic field in a range of 50–80 Oe and frequency of 178 kHz, provided by a commercial generator (RDO HFI 5 KW).

The SAR of the samples was derived from heating rate as following: $SAR = C^*(\Delta T/\Delta t)^*(m_{sample}/m_{mnp})(W.g^1)$, in which C is specific heat of water (4.18 J $g^{-1}K^{-1}mol^{-1}$), m_{sample}/m_{mnp} is the nanoparticle concentration in the fluid, and $(\Delta T/\Delta t)$is the initial slope of the temperature versus time plot. The intrinsic Loss Power (ILP) was also calculated as mentioned in the other publications: $ILP = SAR/(H^2 f)$ [23,24].

2.7. MR images

MR images using L3@PMAO sample as a contrast agent with different concentrations in solution (*ex-vivo*) and in rabbit (*in-vivo*) were taken using MR spectroscopy (Siemens) at frequency of 64 MHz and magnetic field of 1.5 T at Vinh international hospital (Vinh city, Nghe An Province, Vietnam).

For MR images in solution, a series of diluted ferrofluids with iron concentration of 10, 15, 20, 30 and 45 μg/ml was prepared and placed in 2-ml cuvettes. For *in-vivo* MR images in rabbit, 6 ml of ferrofluids was administered into the 8–10 weeks male white rabbits (weighted approximately 2 kg) through their ear veins at a dose of 20 mg/kg body weight [27]. Five minutes before scanning MRI images, these rabbits were anesthetized with ketamine (15 mg kg^{-1}) and diazepam (2 mg kg^{-1}) for 30 min.

The MR images were taken by two different ways: T_1 (spin-lattice) and T_2 (spin-spin). T_1 and T_2-weighted images depend on TR (repetition time) and TE (echo time), respectively. To obtain T_2 weighted images, it is necessary to choose TE value at the time that the contrasts between the two different tissues are strongest. The maximum T_2 value can be obtained at long TE.

EFilm Workstation (Merge Healthcare) was used to determine signal intensity (SI) of the investigating region of the liver, and also other organs (spleen, kidney) of the studied rabbits before and after being injected the ferrofluid with the same diameter or square, in the same slice of T_2 image at each time.

Table 1
Mean size D_{TEM} and saturation magnetization M_s of the samples before and after phase transfer process.

Before phase transfer	D_{TEM} *(nm)* [24]	M_s *(emu/g)* [24]	After phase transfer	D_{TEM} *(nm)*	M_s (emu/g)
M1	8	54	L1@PMAO	10.1	50
M2	10	66	L2@PMAO	13.5	60
M3	13	70	L3@PMAO	16.8	65

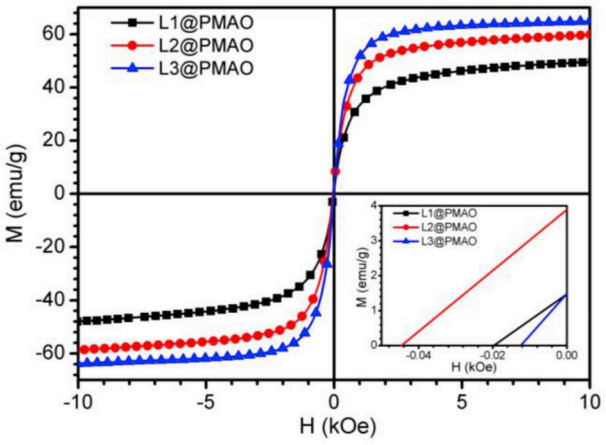

Fig. 3. M(H) curves of ferroliquids (L1@PMAO, L2@PMAO, L3@PMAO)

Table 2
The average particle size (D_{DLS}), PDI index and zeta potential of ferroliquids.

Samples	D_{DLS} (nm)	PDI	Zeta Potential (mV)	D_{DLS} (nm)	PDI	Zeta Potential (mV)
	0 - months			6 - months		
L3@SDS	78.7	0.26	−49.4	126.1	0.72	−16.6
L3@PAA	49.7	0.27	−42.5	177.0	0.75	−12.5
L3@PMAO	80.1	0.17	−40.6	83.54	0.19	−40.9

3. Results and discussion

3.1. Morphological and magnetic behaviors of ferrofluids

In hyperthermia and MRI enhancement, the used ferrofluid should own high homogeneity, good dispersion and high saturation magnetization (M_s). For this reason, the morphology and magnetic behaviors of all prepared samples were tested.

Fig. 2 represents the TEM images and size distribution diagrams of prepared ferroliquids (L1@PMAO, L2@PMAO and L3@PMAO). As seen from Fig. 2, the post-phase transferred samples show good dispersion of magnetic particles with uniform shape and narrow size distribution. The average size of L1@PMAO, L2@PMAO and L3@PMAO samples (estimated from TEM images) are 10.1, 13.5, and 16.8 nm, respectively. Compared to the ones before phase transfer, the particle size of these ferrofluids was increased about 25–30% (Table 1). These evidences have clearly demonstrated that the magnetic particles were fully covered by an additive layer of PMAO.

The magnetic hysteresis loops for ferroliquids are shown in Fig. 3. It can be seen that the saturation magnetization (M_s) of the L1@PMAO, L2@PMAO and L3@PMAO samples are of 50, 60, and 65 emu.g^{-1}, respectively. Moreover, as shown in inset of Fig. 3, the coercivity (H_C) of samples are about 20, 44 and 12 Oe L1@PMAO, L2@PMAO and L3@PMAO samples, respectively. It is well-known that the transition from multi-domain to single domain state of the material can be understood from dependence of H_C versus particle size. In the multi domain state of the material, the H_C will decrease as the grain size increase and the maximum coercivity occurs separates both multidomain and single domain states, therefore from the dependence H_C vs. grain size of our samples, it is believing that our samples possess a single domain nature below 10 nm and above which multi-domain state is expected. The observed variation of coercivity is in consonance with those reported by many researchers [28–30].

The decrease of the saturation magnetization after carrying out the phase transfer by PMAO is probably caused by the decrease of magnetite concentration, and, as a result, of measured magnetic moment in a unit of mass. These values are slightly smaller than that before phase transfer (7–9%) (Table 1), indicating the formation of a non-magnetic thin film covering totally the surface of magnetic nanoparticles [31,32]. All three ferrofluids are well dispersed with homogeneous shape and size, but the sample L3@PMAO with the highest M_s was chosen for further studies in hyperthermia and MRI contrast enhancement applications.

3.2. Stability

For almost biomedical applications, the ferrofluids should remain colloidally stable in aqueous conditions. Therefore, the stability of the as-prepared ferrofluid L3@PMAO was tested by dynamic light scattering technique (Figs. 2S and 3S). The L3@PMAO ferrofluid was stored over time (up to six months) and its stability was compared with that of the ferrofluids coated with SDS and PAA described in our previous works [23,24]. The particle size, PDI and zeta potential of the ferrofluids with different ligands (L3@SDS, L3@PAA, L3@PMAO) right after sample preparation and six-months later were all evaluated and given in Table 2.

Table 3
Proliferation rate (A %) of Sarcoma. 180 in L3@PMAO solution.

Concentration (μg/ml)	*Proliferation rate (A %)*
400	55.6 ± 1.66
200	64.3 ± 7.1
100	91.3 ± 14.4
25	91.3 ± 12.2
12.5	92.1 ± 1.2
6.25	96.6 ± 1.9

As seen from Table 2, the hydrodynamic radius was found to be slightly increased by only 5% for PMAO coating, but strongly increased by 65% for SDS coating and even 261% for PAA coating. At the same time, the PDI indexes were smaller than 0.3 and zeta potentials were higher than – 40 mV for all ferrofluids (right after sample preparation). After six months, it was found that the PDI was increased dramatically (up to more than 0.7) whereas zeta potential was decreased strongly (less than −20 mV) for SDS and PAA coatings; but both kept nearly constant for PMAO coating. In general, the nanoparticles with slight negative charge (zeta potential of – 20 ÷ – 60 mV) [33,34] can minimize their electrostatic adsorption with negatively charged living organisms (i.e., plasma and blood cells). Meanwhile, the PDI value less than 0.3 should be obtained for homogeneous solution of nanoparticles [35]. Therefore, these results have clearly demonstrated that the L3@PMAO ferrofluid was relatively stable even after six months of storage.

In fact, the intrinsic agglomeration of magnetic particles which is resulted from Van Der Waals and magneto-dipole attractions is unavoidable. Therefore, coating the surface of magnetic particles with an organic material is favorable in order to improve their colloidal stability. Obviously, the PMAO polymeric layer has provided a very hard steric barrier which can limit the precipitation of magnetic particles. In addition, the long polymeric chains of PMAO and its high coverage on particle surfaces are supposed to significantly increase such steric repulsion. More importantly, this maleate copolymer must have been deprotonated and/or hydrated in aqueous solutions to electrostatically stabilize the magnetite ferrofluids. For those reasons, the L3@PMAO ferrofluid was found to be stable at room temperature over months. The long-term stability of the ferrofluids in aqueous media will probably offer a great deal of flexibility for their biomedical applications such as hyperthermia and MR imaging. This result is consistent with our visual observations (Fig. 4S).

3.3. In vitro cytotoxicity test by MTT assay method

Iron oxide nanoparticles are intentionally tailored to interact with cells in biomedical applications (i.e., hyperthermia and MRI), though their toxicity should be considered to avoid unwanted adverse effects. The cytotoxicity profile of L3@PMAO ferrofluid toward Sarcoma. 180 (cancer cells) was determined by MTT assay which is very suitable for mammalian cells (Fig. 5S). The cells were incubated with nanoparticles for 24 h with concentrations from 6.25 to 400 μg mL^{-1} in 5% CO_2.

The cell viability in diluted solutions (less than 100 μg mL^{-1}) was estimated to be higher than 90% (Table 3), indicating an ignorable inhibitive effect of magnetic materials. Even at very high concentrations of magnetic liquid (200 and 400 μg mL^{-1}), the cell viability was still as high as 55% and 64%. It was also recommended that the concentration of magnetic nanoparticles beyonds 200 μg mL^{-1} should be avoided in biomedical applications [1].

3.4. Magnetic induction heating

Magnetic fluid hyperthermia has been recently reported to be a very promising technique for cancer treatment. In this technique, the ferrofluids are able to absorb electromagnetic energy, then heat up and destroy localized portions (i.e., tumor cells) in a living body. To evaluate

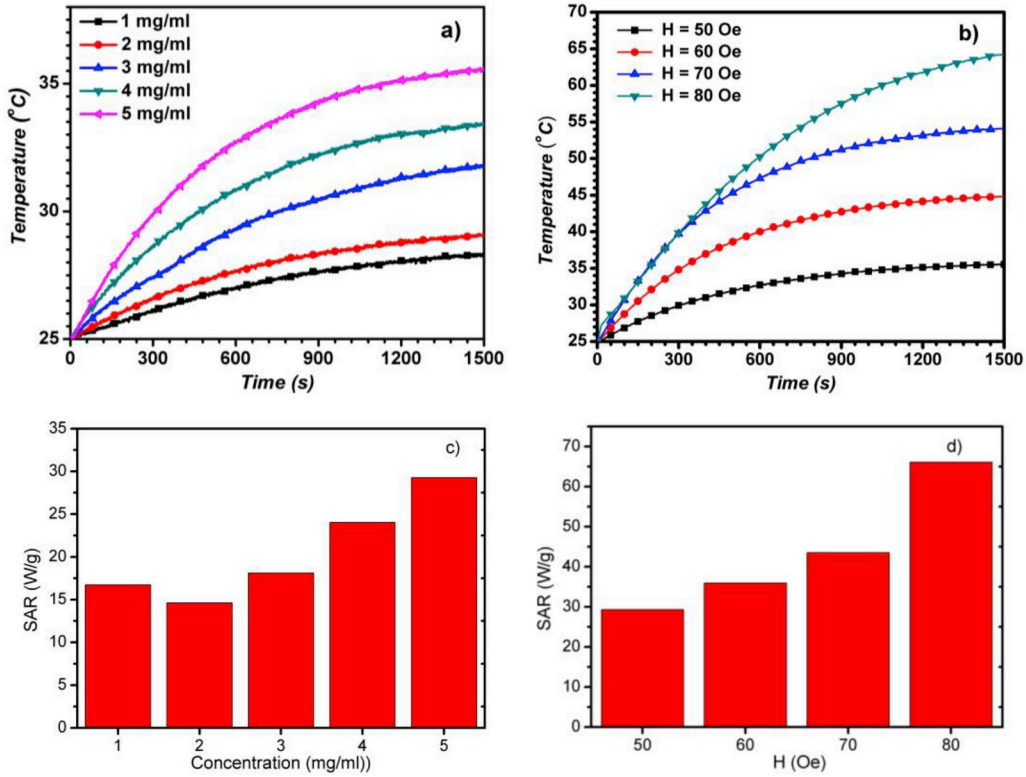

Fig. 4. a) Magnetic heating curves of the L3@PMAO ferrofluid with different concentrations under the external magnetic field of 50 Oe, b) Magnetic heating curves of the L3@PMAO with the concentration of 5 mg/ml at different magnetic fields, c) The SAR values depend on ferrofluid concentration and d) The SAR values depend on magnetic field.

Table 4
Measured temperature (T_{1500s}), Specific Absorption Rate and initial heating rate ($\Delta T/\Delta t$) of the L3@PMAO ferrofluid at concentration of 5 mg/ml at different magnetic field strength values.

Sample	Concentration (mg/ml)	Magnetic field (H, f) (Oe, kHz)	T_{1500s} (^oC)	SAR (W/g)	($\Delta T/\Delta t$) ($^oC/s$)
L3@PMAO	5	50; 178	35.6	29.26	0.035
		60; 178	45.9	35.94	0.043
		70; 178	54.1	43.47	0.052
		80; 178	65.2	66.04	0.079

Table 5
Comparison in specific absorption rate and intrinsic loss power.

Parameters	Current study	Ref. [37]	Ref. [38]	Ref. [39]
D_{TEM}	13 nm	15 nm	15 nm	9 nm
AC field parameters	H = 6.4 kA/m, f = 178 kHz	H = 13 kA/m, f = 100 kHz	H = 12 kA/m, f = 300 kHz	H = 10.3 kA/m, f = 330.3 kHz
Concentration	5 mg/ml	10 mg/ml	15 mg/ml	2 mg/ml
SAR (W/g)	66.04	48	86.87	140.8
ILP (nHm^2kg^{-1})	9.05	2.84	2.03	3.9

the hyperthermic efficiency of one ferrofluid, several important factors such as the Specific Absorption Rate, and the Intrinsic Loss Power should be evaluated. Herein, the magnetic induction heating studies of L3@PMAO ferrofluid were performed at different alternating magnetic fields on the ferrofluid L3@PMAO with different concentrations to find out suitable conditions for hyperthermia applications.

Firstly, the magnetic heating curves of the L3@PMAO ferrofluid were measured at different concentrations (1–5 mg mL^{-1}) under an external magnetic field of 50 Oe (Fig. 4a). The measured temperature value (T_{meas}) was found to be in the range of 28–35 °C after 25 min exposing the samples in magnetic field. These values are much lower than the desirable temperatures in hyperthermic cancer treatments (42–47 °C). Therefore, the magnetic heating curves of the ferrofluid at concentration of 5 mg mL^{-1} were studied at stronger magnetic fields (Fig. 4b). Obviously, the heating rate increases with the concentration as well as magnetic field. As seen from Fig. 4c and Fig. 4d, SAR values increase with increasing magnetic field strength and concentration. The T_{meas} of 45.9 °C was obtained at magnetic field of 60 Oe and ferrofluid concentration of 5 mg mL^{-1} (Table 4). The exact heating mechanism of hyperthermia is actually not that simple and still rests controversial until now. Indeed, it is suggested that there are four main phenomena could be involved in this magnetic heating process, including hysteresis loss (orientation towards external field), Foucault (eddy current), Brownian relaxation (momentum of single moments) and Néel relaxation (momentum of total moment). Nevertheless, the two later ones are supposed to contribute more to hyperthermia [36].

SAR values of the ferrofluids coated with SDS, PAA and PMAO were compared to each other when measured at concentration of 5 mg/ml, magnetic field of 80 Oe (Fig. 6S). It was found that at the same concentration of 5 mg/ml and magnetic field of 80 Oe, the L3@PMAO ferrofluid had a higher SAR (66 W g^{-1}) compared to L3@SDS sample (48 W g^{-1}) [37,38] but smaller than that of L3@PAA sample (86 W g^{-1}) [37,38] (Table 5). Indeed, the SAR values for magnetite systems are often found in the range from several tens to hundreds W.g^{-1}. More importantly, the intrinsic loss power of L3@PMAO was also estimated to be 9.05 nHm^2kg^{-1} which was higher compared with previously reported works [23,24,37–39] (Table 5). Clearly, the ferrofluid with a medium SAR value, but high ILP and enhanced stability as obtained here is very promising for tumor hyperthermia.

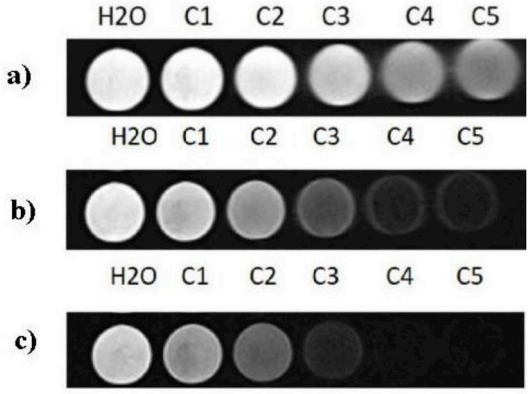

Fig. 5. T_2 -weighted MRI of L3@PMAO at different conditions, (a) TE = 11 ms, TR = 3970 ms; (b) TE = 34 ms, TR = 3970; (c) TE = 91 ms, TR = 3970 ms. (H_2O, C1, C2, C3, C4 and C5 are at concentration of 0, 10, 15, 20, 30 and 45 μg iron/ml, respectively).

3.5. MRI contrast enhancement

MRI has been one of the most effective tools for cancer diagnosis in recent years. In this technique, different soft tissues in a living body injected with a ferrofluid will be distinguished by the different relaxation times T_2 of the magnetic moments entrapped within these tissues. A high-resolution MR image will be obtained with high contrast degree if the used ferrofluid can provide significant tissue-to-tissue variation in T_2 values. Here, the contrast efficiency of L3@PMAO ferrofluid for MR imaging will be investigated in both *in-vitro* and *in-vivo* conditions.

3.5.1. In-vitro relaxivity measurement

In-vitro MR imaging using L3@PMAO as contrast agent was performed in water. T_2 – weighted MR images were acquired at different iron concentrations (0–45 μg iron per milliliter) and depicted in Fig. 5. The images were captured at TR of 3970 ms while three different values of TE were tested to find out the best contrast degree. It is obviously that the considerable contrast degree was obtained from one to another sample even when the difference in their concentrations was very small. The T_2 MR signal became darker with increasing concentration of the ferrofluid, indicating higher transverse relaxation rate. Here, only first observations on relaxivity are given and further details on transverse relaxation rates will be evaluated in our future studies. As expected, this contrast degree was also improved with increasing TE and the best contrast was obtained at TE of 91 ms. Therefore, all *in-vivo* MR images on rabbit will be later captured at this condition.

According to Solomon-Bloembergen-Morgan theory, the T_2-weighted contrast ability of magnetic ferrofluids strongly depends on magnetic forces acting on particles as well as their contact area with water molecules [40]. Probably, the L3@PMAO ferrofluid with diameter of only 13 nm and M_s up to 65 emu.g^{-1} must have exhibited considerable relaxivities. Especially, the high relaxivity of our sample could have also contributed to the fact that the hydrophilic groups on the surface of L3@PMAO significantly improved the solubility of particles in aqueous solution, thus enhanced the contact area between water molecules and magnetic nanoparticles [14]. On the other hand, the use of PMAO as ligand is beneficial in not only improving colloidal stability of the ferrofluids but also enhancing contrast degree in MRI images.

3.5.2. In-vivo relaxivity measurement

Ferrofluids are often chosen as contrast agent in MRI applications due to their ability to reach bone marrow, blood circulation [41] and be recognized by reticuloendothelial system [42]. Herein, the *in-vivo* MR images of the rabbit before and 30 min after being injected with 10 ml of L3@PMAO ferrofluid (5 mg mL^{-1}) in T_2 map were recorded at different TE values (11, 34, and 91 ms). Indeed, the ferrofluid which was directly injected through veins should have circulated through blood vessels and entered many different organs in the rabbit body. Nevertheless, the accumulation of particles is more often found in liver due to the uptake of mononuclear phagocyte systems in this organ [43,44]. Thus, the liver of mice was chosen as the region of interest and performed T_2-weighted MR imaging.

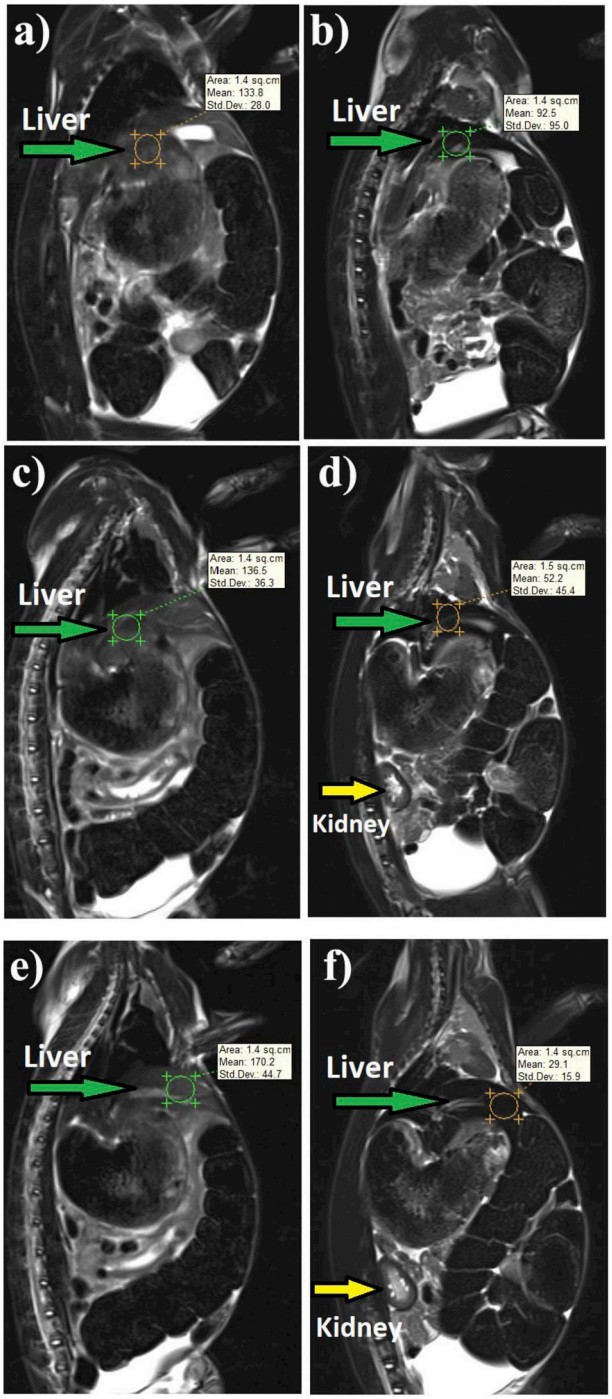

Fig. 6. T_2 weighted images of the animal before injected (a), (c) and (e); 30 min after injected by L3@PMAO sample (b), (d) and (f). (a,b) TE = 11 ms, TR = 3970 ms; (c,d) TE = 34 ms, TR = 3970; (e,f) TE = 91 ms, TR = 3970 ms.

Fig. 6 showed the MR images of a rabbit acquired before and after the administration of the ferrolfuid. It can be seen from Fig. 6, the quality of MR images of some organs (heart, liver, and kidney) is much improved with higher brightness as L3@PMAO ferroliquid is used. In detail, the T_2-weighted signal intensity in the liver tissues was approximately 1.45,

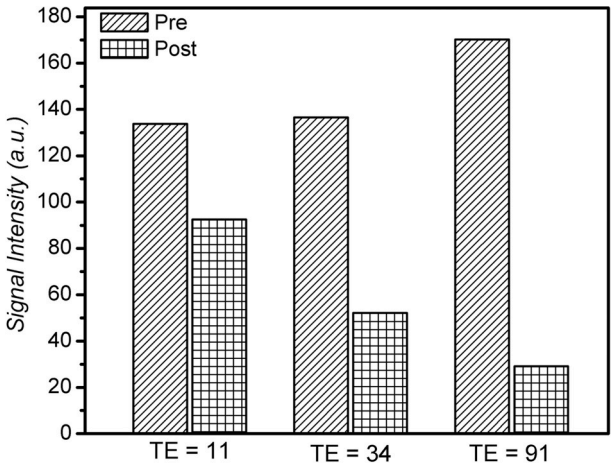

Fig. 7. Bar graph showed the mean signal intensity of T2-weighted image using different TE values.

2.6 and 5.85 times higher than that before the administration of the ferrofluid at TE of 11, 34 and 91 ms, respectively. These results indicated that L3@PMAO samples can be used as an effective contrast agent for T_2-weighted MR imaging. This is benefited from the characteristic feature of Fe_3O_4 magnetic nanoparticles in enhancing the transverse relaxation rate (R2), therefore, reducing relaxation time T_2 and T_2*.

The T_2-weighted gradient-echo MR bar chart at different TE values of the L3@PMAO ferrofluid is shown in Fig. 7. It can be seen that there is a significant decrease in signal intensity at liver tissues accompanied with ferrofluid compared to the case without ferrofluid.

The reduction of the signal intensity in the liver demonstrated that the magnetic nanoparticles have been delivered and trapped in this organ. This result opens a very promising ability to accurately determine liver tumors [45–47]. More details on the uptake mechanism of nanoparticles in liver were mentioned in previous works [44,48]. Actually, it is not really easy to detect liver cancer at early stages. Up to now, the available MRI contrast agents are only able to detect liver tumor at the diameter more than 5 cm when the cancer is already aggressive and hard to be removed by surgery or treated by chemotherapy. Probably, the use of magnetic particles with such high contrast degree will much improve the quality of MRI images and enable early diagnosis of liver cancer.

4. Conclusion

In conclusion, a high-quality ferrofluid based on magnetite particles was achieved by thermal decomposition method with using PMAO as a novel phase transfer ligand. This ligand could improve the ferrofluid stability up to as long as 6 months. At concentration of only 5 mg/ml, the SAR value was relatively high of 66.04 W/g measured at magnetic field amplitude of 80 Oe and frequency of 178 kHz. The MR images in solution and in rabbit using the prepared PMAO-coated Fe_3O_4 magnetic nanoparticles had the best contrast effect on T_2 weighted maps. We also determined that the magnetic nanoparticles are trapped mainly in the liver, in which the particles enhance transverse relaxation rate (R2), reflecting the possibility of using Fe_3O_4 magnetic nanoparticles in T_2 weighted MRI. Probably, the synthesized ferrofluid would provide a feasible and cost effective tool for cancer diagnosis and treatment in the future.

Declaration of competing interest

The authors declare that there is no conflict of interest in this work. Kind regards,

Acknowledgment

This research is funded by Vietnam National Foundation for Science and Technology Development (NAFOSTED) under grant number 103.02-2017.339.

Appendix A. Supplementary data

Supplementary data to this article can be found online at https://doi.org/10.1016/j.matchemphys.2020.122762.

References

[1] G.S. Ningombam, R.S. Ningthoujam, S.N. Kalkura, N.R. Singh, Induction heating efficiency of water-dispersible $Mn_{0.5}Fe_{2.5}O_4$@YVO_4:Eu^{3+} magnetic-luminescent nanocomposites in an acceptable ac magnetic field: hemocompatibility and cytotoxicity studies, J. Phys. Chem. B 122 (2018) 6862–6871.
[2] X. Meng, H.C. Seton, le T. Lu, I.A. Prior, N.T. Thanh, B. Song, Magnetic CoPt nanoparticles as MRI contrast agent for transplanted neural stem cells detection, Nanoscale 3 (2011) 977–984.
[3] Le Trong Lu, Le Duc Tung, James Long, David Garth Fernigef, Nguyen Thi Kim Thanh, Facile synthesis of stable, water-soluble magnetic CoPt hollow nanostructures assisted by multi-thiol ligands, J. Mater. Chem. 19 (2009) 6023–6028.
[4] Jae-Hyun Lee, Yong-Min Huh, Jun Young-wook, Seo Jung-wook, Jang Jung-tak, Song Ho-Taek, Sungjun Kim, Eun-Jin Cho, Yoon Ho-Geun, Suh Jin-Suck, Cheon Jinwoo, Artificially engineered magnetic nanoparticles for ultra-sensitive molecular imaging, Nat. Med. 13 (2007) 95–99.
[5] Seok Seo Won, Hyung Lee Jin, Xiaoming Sun, Yoriyasu Suzuki, Davidmann, Zhuang Liu, Masahiro Terashima, Philipc Yang, Michael V. Mcconnell, Dwight G. Nishimura, Hongjie Dai, FeCo/graphitic-shell nanocrystals as advanced magnetic-resonance-imaging and near-infrared agents, Nat. Mater. 5 (2006) 971–976.
[6] R.K. Gilchrist, W.D. Shorey, R.C. Hanselman, J.C. Parrott, C.B. Taylor, Selective inductive heating of lymph nodes, Ann. Surg. 146 (1957) 596–606.
[7] R.T. Gordon, J.R. Hines, D. Gordon, Intracellular hyperthermia a biophysical approach to cancer treatment via intracellular temperature and biophysical alterations, Med. Hypotheses 5 (1979) 83–102.
[8] N.X. Phuc, N.A. Tuan, N.C. Thuan, V.A. Tuan, L.V. Hong, Magnetic nanoparticles as smart heating mediator for hyperthermia and sorbent regeneration, Adv. Mater. Res. 55–57 (2008) 27–32.
[9] Rudolf Hergt, Silvio Dutz, Magnetic particle hyperthermia—biophysical limitations of a visionary tumour therapy, J. Magn. Magn Mater. 311 (2007) 187–192.
[10] D. H Han, J.P. Wang, H.L. Luo, Crystallite size effect on saturation magnetization of fine ferrimagnetic particles, J. Magn. Magn Mater. 136 (1994) 176–182.
[11] R. Jin, B. Lin, D. Li, H. Ai, Superparamagnetic iron oxide nanoparticles for MR imaging and therapy: design considerations and clinical applications, Curr. Opin. Pharmacol. 18 (2014) 18–27.
[12] N. Lee, T. Hyeon, Designed synthesis of uniformly sized iron oxide nanoparticles for efficient magnetic resonance imaging contrast agents, Chem. Soc. Rev. 41 (2012) 2575–2589.
[13] Ereath Beeran Ansar, Fernandez Francis Boniface, P.R. Harikrishna Varma, Self-controlled hyperthermia & MRI contrast enhancement via iron oxide embedded hydroxyapatite superparamagnetic particles for theranostic application, ACS Biomater. Sci. Eng. 5 (2019) 106–113.
[14] J. Xiao, G. Zhang, J. Qian, X. Sun, J. Tian, K. Zhong, D. Cai, Z. Wu, Fabricating high-performance T2-weighted contrast agents via adjusting composition and size of nanomagnetic iron oxide, ACS Appl. Mater. Interfaces 10 (2018) 7003–7011.
[15] Qinlu Zhang, Qian Liu, Menghan Du, Alphons Vermorken, Yali Cui, Lixia Zhang, Lili Guo, Le Ma, Mingwei Chen, Cetuximab and Doxorubicin loaded dextran-coated Fe_3O_4 magnetic nanoparticles as novel targeted nanocarriers for non-small cell lung cancer, J. Magn. Magn Mater. 481 (2019) 122–128.
[16] Fei Wang, Xinshi Li, Wentao Li, Hua Bai, Yue Gao, Jiahua Ma, Wei Liu, Xi Guangcheng, Dextran coated Fe_3O_4 nanoparticles as a near-infrared laser-driven photothermal agent for efficient ablation of cancer cells in vitro and in vivo, Mater. Sci. Eng. C 90 (2018) 46–56.
[17] Yongling Ding, Z. Shen Shirley, Huadong Sun, Kangning Sun, Futian Liu, Yushi Qi, Jun Yan, Design and construction of polymerized-chitosan coated Fe_3O_4 magnetic nanoparticles and its application for hydrophobic drug delivery, Mater. Sci. Eng. C 48 (2015) 487–498.
[18] Kunal Patel, Behin Sundara Raj, Chen Yan, Lou Xia, Novel folic acid conjugated Fe_3O_4-ZnO hybrid nanoparticles for targeted photodynamic therapy, Colloids Surf. B Biointerfaces 150 (2017) 317–325.
[19] K. Oihane, Arriortua Eneko Garaio, Borja Herrero de la Parte, Maite InsaustiLuis Lezama, Fernando Plazaola, Jose Angel García, Jesús M. Aizpurua, Maialen Sagartzazu, Mireia Irazola, Nestor Etxebarria, Ignacio García-Alonso, A. Saiz-López, José Javier Echevarria-Uraga, Antitumor magnetic hyperthermia induced by RGD-functionalized Fe_3O_4 nanoparticles, in an experimental model of colorectal liver metastases, Beilstein J. Nanotechnol. 7 (2016) 1532–1542.
[20] A.P. Khandhar, R.M. Ferguson, K.M. Krishnan, Monodispersed magnetite nanoparticles optimized for magnetic fluid hyperthermia: implications in biological systems, J. Appl. Phys. 109 (2011) 31.

[21] Swati Biswas, Namita S. Dodwadkar, Rupa R. Sawant, Vladimir P. Torchilin, Development of the novel PEG-PE-based polymer for the reversible attachment of specific ligands to liposomes: synthesis and in vitro characterization, Bioconjugate Chem. 22 (10) (2011) 2005–2013.
[22] G. Jiang, J. Pichaandi, N.J. Johnson, R.D. Burke, F.C. Van Veggel, An effective polymer cross-linking strategy to obtain stable dispersions of upconverting NaYF4 nanoparticles in buffers and biological growth media for biolabeling applications, Langmuir 28 (2012) 3239–3247.
[23] Vuong Thi Kim Oanh, Tran Dai Lam, Vu Thi Thu, Le Trong Lu, Pham Hong Nam, Le The Tam, Do Hung Manh, Nguyen Xuan Phuc, A novel route for preparing highly stable Fe_3O_4 fluid with poly(acrylic acid) as phase transfer ligand, J. Electron. Mater. 45 (2016) 4010–4017.
[24] Thi Kim Oanh Vuong, Tran Dai Lam, Trong Lu Le, Duy Viet Pham, Hong Nam Pham, Thi Hong Le Ngo, Hung Manh Do, Xuan Phuc Nguyen, Synthesis of high-magnetization and monodisperse Fe_3O_4 nanoparticles via thermal decomposition, Mater. Chem. Phys. 163 (2015) 537–544.
[25] J. Carmichael, W.G. DeGraff, A.F. Gazdar, J.D. Minna, J.B. Mitchell, Evaluation of a tetrazolium-based semiautomated colorimetric assay: assessment of radiosensitivity, Canc. Res. 47 (1987) 943–946.
[26] T. Xu, C. Niu, X. Zhang, M. Dong, β-Ecdysterone protects SH-SY5Y cells against β-amyloid-induced apoptosis via c-Jun N-terminal kinase- and Akt-associated complementary pathways, Lab. Invest. 98 (4) (2018) 489–499.
[27] B. Feng, R.Y. Hong, L.S. Wang, L. Guo, H.Z. Li, J. Ding, Y. Zheng, D.G. Wei, Synthesis of Fe_3O_4/APTES/PEG diacid functionalized magnetic nanoparticles for MR imaging, Colloids Surf A Physicochem Eng Asp 328 (2008) 52–59.
[28] K. Srinivasa Rao, S.V. Ranga Nayakulu, M. Chaitanya Varma, G.S.V.R.K. Choudary, K.H. Rao, Controlled phase evolution and the occurrence of single domain $CoFe_2O_4$ nanoparticles synthesized by PVA assisted sol-gel method, J. Magn. Magn Mater. 451 (2018) 602–608.
[29] Vinod Kumar, Anu Rana, M.S. Yadav, R.P. Pant, Size-induced effect on nano-crystalline $CoFe_2O_4$, J. Magn. Magn Mater. 320 (2008) 1729–1734.
[30] W.S. Chiu, S. Radima, R. Abd-Shukor, M.H. Abdullah, P.S. Khiew, Tunable coercivity of $CoFe_2O_4$ nanoparticles via thermal annealing treatment, J. Alloys Compd. 459 (2008) 291–297.
[31] T.T. Dung, T.M. Danh, L.T.M. Hoa, D.M. Chien, N.H. Duc, Structural and magnetic properties of starch-coated magnetite nanoparticles, J. Exp. Nanosci. 4 (2009) 259–267.
[32] Saikia Chinmayee, Anowar Hussain, Ramteke Anand, K. Sharma Hemanta, K. Maji Tarun, Crosslinked thiolated starch coated Fe_3O_4 magnetic nanoparticles: effect of montmorillonite and crosslinking density on drug delivery properties, Starch Staerke 66 (2014) 760–771.
[33] D.C. Jeffrey, K.P. Anil, Chapter 6: zeta potential measurement, in: Characterization of Nanoparticles Intended for Drug DeliveryScientia Pharmaceutica, 2011.
[34] Zhiping Zhang, Feng Si-Shen, Nanoparticles of poly(lactide)/vitamin E TPGS copolymer for cancer chemotherapy: synthesis, formulation, characterization and in vitro drug release, Biomaterials 27 (2006) 262–270.
[35] R.P. Araújo-Neto, E.L. Silva-Freitas, J.F. Carvalho, T.R.F. Pontes, K.L. Silva, I.H. M. Damasceno, E.S.T. Egito, Ana L. Dantas, Marco A. Morales, Artur S. Carriço, Monodisperse sodium oleate coated magnetite high susceptibility nanoparticles for hyperthermia applications, J. Magn. Magn Mater. 364 (2014) 72–79.
[36] Pham Thanh Phong, Luu Huu Nguyen, Do Hung Manh, In-Ja Lee, Nguyen Xuan Phuc, Computer simulations of contributions of Néel and Brown relaxation to specific loss power of magnetic fluids in hyperthermia, J. Electron. Mater. 46 (2017) 2393–2405.
[37] E. Lima Jr., E. De Biasi, M. Vasquez Mansilla, M.E. Saleta, M. Granada, H. E. Troiani, F.B. Effenberger, L.M. Rossi, H.R. Rechenberg, R.D. Zysler, Heat generation in agglomerated ferritenanoparticles in an alternating magnetic field, J. Phys. D Appl. Phys. 46 (2013), 045002 - 045015.
[38] Yury V. Kolen'ko, Manuel Bañobre-López, Carlos Rodríguez-Abreu, Enrique Carbó-Argibay, Alexandra Sailsman, Yolanda Piñeiro-Redondo, M. Fátima Cerqueira, Dmitri Y. Petrovykh, Kirill Kovnir, Oleg I. Lebedev, José Rivas, Large-scale synthesis of colloidal Fe_3O_4 nanoparticles exhibiting high heating efficiency in magnetic hyperthermia, J. Phys. Chem. C 118 (2014) 8691–8701.
[39] Ganeshlenin Kandasamy, Atul Sudame, Piyush Bhati, Anindita Chakrabarty, Dipak Maity, Systematic investigations on heating effects of carboxyl-amine functionalized superparamagnetic iron oxide nanoparticles (SPIONs) based ferrofluids for in vitro cancer hyperthermia therapy, J. Mol. Liq. 256 (2018) 224–237.
[40] Daniel L.J. Thorek, Andrew Tsourkas, Size, charge and concentration dependent uptake of iron oxide particles by non-phagocytic cells, Biomaterials 29 (2008) 3583–3590.
[41] M.R. Bashir, L. Bhatti, D. Marin, R.C. Nelson, Emerging applications for ferumoxytol as a contrast agent in MRI, J. Magn. Reson. Imag. 41 (2015) 884–898.
[42] Yi-Xiang J. Wang, Shahid M. Hussain, Gabriel P. Krestin, Superparamagnetic iron oxide contrast agents: physicochemical characteristics and applications in MR imaging, Eur. Radiol. 11 (2001) 2319–2331.
[43] Lijiao Yang, Lengceng Ma, Jingyu Xin, Li Ao, Chengjie Sun, Wei Ruixue, Bin W. Ren, Chen Zhong, Hongyu Lin, Jinhao Gao, Composition tunable manganese ferrite nanoparticles for optimized T2 contrast ability, Chem. Mater. 29 (2017) 3038–3047.
[44] Yi-Nan Zhang, Poon Wilson, J. Tavares Anthony, D. McGilvray Ian, C.W. Chan Warren, Nanoparticle–liver interactions: cellular uptake and hepatobiliary elimination, J. Contr. Release 240 (2016) 332–348.
[45] Alexander M. Demin, Alexandra G. Pershina, Artem S. Minin, V. Alexander, Mekhaev, V. Vladimir, Sofiya P. Lezhava Ivanov, Alexandra A. Zakharova, Iliya V. Byzov, Mikhail A. Uimin, P. Victor, a.L.M. Krasnov, Ogorodova, PMIDA-modified Fe_3O_4 magnetic nanoparticles: synthesis and application for liver MRI, Langmuir 34 (2018) 3449–3458.
[46] Q. Chen, W. Shang, C. Zeng, K. Wang, X. Liang, C. Chi, J. Yang, C. Fang, J. Tian, Theranostic imaging of liver cancer using targeted optical/MRI dual-modal probes, Oncotarget 8 (2017) 32741–32751.
[47] R.A. Revia, M. Zhang, Magnetite nanoparticles for cancer diagnosis, treatment, and treatment monitoring: recent advances, Mater. Today 19 (2016) 157–168.
[48] Kim M. Tsoi, Sonya A. MacParland, Xue-Zhong Ma, Vinzent N. Spetzler, Juan Echeverri, Ben Ouyang, Saleh M. Fadel, Edward A. Sykes, Nicolas Goldaracena, Johann M. Kaths, John B. Conneely, Benjamin A. Alman, Markus Selzner, Mario A. Ostrowski, Oyedele A. Adeyi, Anton Zilman, Ian D. McGilvray, Warren C. W. Chan, Mechanism of hard-nanomaterial clearance by the liver, Nat. Mater. 15 (2016) 1212.